COMPLETE DEVELOPMENT OF THE TURBULENT DISTRIBUTION OF VELOCITY IN SMOOTH DUCTS

By

H. Reichardt, Gottingen

Translated by
H. H. Schweizer
Assistant Professor
Civil Engineering Department
Colorado A and M College
Fort Collins, Colorado

CER56HHS10

Foreword: The following article has been translated from Zeitschrift für angewandte Mathematik und Mechanik, Band 31, Juli, 1951 Heft 7 (pp. 208-219 incl.) Every effort has been made to retain the characteristics and continuity of the original article.

COMPLETE DEVELOPMENT OF THE TURBULENT DISTRIBUTION OF VELOCITY IN SMOOTH DUCTS

By H. Reichardt, Göttingen
(From the Max Planck-Institute for Flow Research)

Translated by
H. H. Schweizer
Assistant Professor
Civil Engineering Department
Colorado A and M College
Fort Collins, Colorado

Based on experimental investigations of turbulent exchange of momentum, an equation for the velocity distribution of turbulent flow in pipes and canals was developed. This equation gives a complete representation of the velocity distribution; that is, it is valid for the region immediate to the boundary as well as for the middle part of the cross-section of flow.

1. STATEMENT OF THE PROBLEM

Thus far, investigations of turbulent flow in pipes, canals, and plane surfaces have shown that the velocity profile approaches a logarithmic distribution. The evaluation of these investigations with the aid of dimensional analysis results in the following turbulent boundary law:

$$\frac{\bar{u}}{u^*} = \frac{1}{\kappa} \ln \eta + C \qquad (1)$$

Here $\bar{u}$ is the mean velocity a distance y from the surface, $u^* = \sqrt{\tau_0/\rho}$ the shear stress velocity, τ_0 the wall shear, ρ the density of the medium, $\eta = \frac{yu^*}{\nu}$ the dimensionless distance from the boundary written in the form of a characteristic Reynolds number, and $\nu = \frac{\mu}{\rho}$ the kinematic viscosity. κ and C are constants.

The development of the above boundary law carries the assumption that the turbulent shear stress is practically of the same magnitude everywhere near the boundary as the wall shear τ_0 . Equation (1) is therefore only valid for a thin layer near the boundary. On the other hand, this layer cannot be too thin because the turbulent condition disappears in the immediate vicinity of the boundary, if for no other reason than continuity. The theory thus far is then limited on both sides to a small region.

As is known, the boundary law is still valid for greater distances from the boundary where the turbulent shear τ_t is considerably different from the wall shear stress τ_0 . This is without doubt of practical importance. However, when considered from the theoretical viewpoint, the validity of an equation outside the range of its basic assumptions is unsatisfactory as long as no sound physical explanation for this fact has been established.

Only toward the middle of the cross-section of flow noticeable deviations appear from the boundary law, and the actual velocities are greater than those calculated by Eq. (1). Even if these "additional velocities on the inner region" (which we will designate by u_i) are small, nevertheless it is of fundamental significance that here the dimensionless velocity does not only directly depend on η but also on the distance from the boundary. A satisfactory representation of these specific relationships on the inner region of the friction layer is as yet lacking.

The writer has therefore set before him the problem to fill in the previously discussed gaps of the theory. First, the boundary law shall be completed by representation of the distribution of velocity in the laminar boundary layer. Then we will clear up the dependence of the velocity of flow within the friction layer upon the distance from the boundary and/or center distance and describe this by an equation.

We limit our considerations to the type of fully developed flow with pressure drop as is observed in pipes or canals.

2. FUNDAMENTAL OBSERVATIONS

If we speak here of a complete representation of the turbulent velocity profile, it does not mean a complete solution of the problem of turbulent distribution of velocity. Exact solutions in turbulence research can only be given if and when the problem of turbulence is solved as such; that is, when (as, for example, in viscous flows) the physical problem can be traced back to purely mathematical assignments. The research in turbulence is, however, still far from this highest level of development. At the most, one can assist himself by working with hypotheses, the usefulness of which the experiment must decide.

Of the efforts to date to lay a theoretical foundation in research of turbulence, (most important are) Prandtl's mixing length hypothesis and v. Karman's similarity hypothesis. As far as pipe flow is concerned, both hypotheses led to a nearly logarithmic distribution of velocity. We must, however, make clear that this boundary law is in no way a binding consequence of the theory about the behavior of the eddies or about the similarity of eddy motion. The only essential assumption for the numerical results was that the mixing length ℓ, defined by the expression $\sqrt{\frac{\tau_t}{\rho}} \Big/ \frac{d\bar{u}}{dy}$, increases linearly with distance from the boundary. This assumption seemed plausible but was, however, not a logical consequence of that hypothesis; so the scientific advancement did not rest in the hypotheses themselves but in a plausible assumption of a helpful idea which could be verified by experiment.

For further advancement of the theory it seemed to us practicable to avoid any speculative considerations and to base the basic premise necessary for the derivations directly on experience. Through formulative reproduction (which is not accomplished without vision) of the test results, naturally a certain error is introduced in the arithmetic expression. In any case, such an inexactly reproduced condition is a better base for the theory than a purely hypothetical premise.

For the investigation at hand we will use the exchange coefficient A as an essential concept. It is defined by the equation

$$\tau_t = A \frac{d\bar{u}}{dy} \tag{2}$$

where τ_t is the turbulent shear stress.[1] The turbulent mixing coefficient is the formula analog of the molecular coefficient of viscosity whose equation of definition is $\tau_m = \mu \frac{d\bar{u}}{dy}$. The coefficient A does not only have a formal, but also an essentially physical meaning, because the question of relationship between the turbulent shear stress τ_t and viscous shear stress τ_m (that is, the relationship $\frac{A}{\mu}$) has a direct physical sense. Therefore in almost all turbulence investigations, and especially so in the consideration at hand, A plays an essential role.

We begin with our investigation using the following identity relation

$$\frac{d\left(\frac{u}{u^*}\right)}{d\eta} = \frac{\frac{du}{dy}}{\left(\frac{du}{dy}\right)_0} = \frac{\tau_m}{\tau_0} \tag{3}$$

---

1 The application of the mixing length concept would be impractical because the velocity gradient would not be eliminated by the representation of the relationship τ_t/τ_m. Further, for the flows treated here, there appears the well known difficulty that the mixing length leads to a singularity in the axis of symmetry. Considering the linear behavior of the shear stress as well as the velocity gradient (see Fig. 4) we have for the middle region $\ell = \sqrt{\frac{\tau_t}{\rho}} \Big/ \frac{d\bar{u}}{dy} \sim \frac{\sqrt{z}}{z} \sim \frac{1}{\sqrt{z}}$, where z denotes the distance from the center. ℓ therefore tends to infinity as $z \rightarrow 0$.

(The index 0 denotes the value of the velocity gradient appearing at the surface relative to the viscous shear stress τ_m.)[2] By verifying Eq (3) one is easily convinced that the differential quotient of the dimensionless velocity by the dimensionless distance from the boundary signifies nothing other than the relationship of the velocity gradient at position y to the corresponding gradient at the wall.

We introduce the total shear stress τ :

$$\tau = \tau_m + \tau_t = (\mu + A)\frac{du}{dy} \tag{4}$$

By substituting this equation into Eq (3) it follows that

$$\frac{d\left(\frac{u}{u^*}\right)}{d\eta} = \frac{\frac{\tau}{\tau_0}}{1+\frac{A}{\mu}} \tag{5}$$

We can see from Eq (5) that the dimensionless distribution of velocity depends on the parameters $\frac{\tau}{\tau_0}$ and $\frac{\tau_t}{\tau_m} = \frac{A}{\mu}$. In the fully developed flow with pressure drop, which we will consider in the following, τ/τ_0 is known and equal to $1 - \frac{y}{r}$ (where y is the distance to the boundary and r is the radius of the pipe or canal). Therefore, our problem reduces itself to the question of the dependence of the exchange coefficient on the distance to the boundary and the Reynolds Number.

As we already mentioned, we can no more calculate the exchange coefficient from the practically unexplored turbulence structure than we can calculate the mixing length or any other helpful concept. We have therefore determined the dimensionless exchange coefficient $\frac{A}{\mu\eta_r}$ by experiment ($\eta_r = \frac{ru^*}{\nu}$). This

---

2 From now on we omit the mean value dash above u if a confusion of u with the instantaneous value $u = \bar{u} + u'$ is not to be feared.

experimentally determined function (see Fig. 5) will enter our calculations later on.

3. THE BOUNDARY LAW

It is relatively easy to determine the exchange coefficient near the boundary from the measured distribution of velocity. Nikuradse[3] has already carried out such a determination of A . His measurements showed that near the boundary

$$\frac{A}{\mu \eta_r} = K \frac{y}{r} \tag{6}$$

(the proportionality coefficient K is about 0.4). Farther away (approximately above $\frac{y}{r} = 0.10$) $\frac{A}{\mu \eta_r}$ increases less than linearly with $\frac{y}{r}$. The investigations of Nikuradse also give information about this behavior. (However, the values above $\frac{y}{r} \simeq 0.8$ are uncertain. (For more details see Section 4.)).

Relative to the region of validity of Eq (6) nothing definite is known as far as small distances from the surface are concerned. It is only definite that Eq (6) can no longer be valid in the immediate vicinity of the boundary because the turbulent exchange there disappears for reasons of continuity, and the liquid moves laminarly parallel to the surface.

Since the continuity is responsible for the suppression of the turbulence at the boundary, we can obtain a relation for the decay of A from the equations of continuity. The condition for continuity of the velocity fluctuations u' (parallel to boundary) and v' (perpendicular to boundary) is as follows:

$$\frac{\partial v'}{\partial y} = -\frac{\partial u'}{\partial x} \tag{7}$$

---

[3] J. Nikuradse, Gesetzmässigkeiten der turbulenten Strömung in glatten Rohren. VDI-Forschungsheft 356, 1932

If we denote the relation $\frac{u'}{\bar{u}}$ by α, then we can express u' as:

$$u' = \alpha \bar{u} = \alpha \left(\frac{d\bar{u}}{dy}\right)_0 y \tag{8}$$

where α represents a function of time and the x coordinate. If we introduce Eq (8) into Eq (7), then follows:

$$v' = -\frac{\partial \alpha}{\partial x}\left(\frac{d\bar{u}}{dy}\right)_0 \frac{y^2}{2} \tag{9}$$

Although we have to assume a linear increase of u' with y (corresponding to the linear increase of $\bar{u}$ with y) as a first approximation, it follows from conditions of continuity that $v' \sim y^2$. From this it follows that

$$\tau_t = -\rho \overline{u'v'} = 0.25 \rho \frac{\partial \bar{\alpha}^2}{\partial x}\left(\frac{d\bar{u}}{dy}\right)_0^2 y^3 \tag{10}$$

for the turbulent shear stress.

For the exchange coefficient in proximity to the boundary we then obtain:

$$\frac{A}{\mu} = 0.25 \frac{\partial \bar{\alpha}^2}{\partial\left(\frac{x}{r}\right)}\left(\frac{yu^*}{\nu}\right)^3 \tag{11}$$

Accordingly, the exchange coefficient is proportional to η^3 (to be sure, here we can make no statement about the magnitude of the factor of proportionality). This signifies an extraordinarily low increase of A for small values of η. The first as well as the second derivative of A with respect to η disappears as the boundary. Only the third derivative has a finite value.*

---

* Comments by the critics.

In the derivation at hand the criticism is that the third fluctuation component w' was neglected. In this simplification, as Eq (11) shows, $\frac{A}{\mu} \sim \eta^3$ when $\frac{\partial \bar{\alpha}^2}{\partial x} \sim \frac{\partial \bar{u'^2}}{\partial x} \neq 0$. But this condition is only satisfied in flow which is not fully developed.

If the w' component is considered and fully developed flow assumed, one obtains instead of Eq (11):

$$\frac{A}{\mu} = \frac{1}{2\,u^{*2}}\left(\frac{\partial u'}{\partial \eta}\right)_0 \frac{\partial}{\partial \xi}\left(\frac{\partial w'}{\partial \eta}\right)_0 \eta^3 \tag{11a}$$

where $\xi = \frac{z u^*}{\nu}$ The question arises whether $\left(\frac{\partial u'}{\partial \eta}\right)_0$ and $\frac{\partial}{\partial \xi}\left(\frac{\partial w'}{\partial \eta}\right)_0$ are correlated. In case these two expressions are entirely uncorrelated, then it follows that the exchange coefficient does not increase with η^3 but with a higher power of η.

We arrive then at the following result: If the behavior of the exchange coefficient in proximity to the boundary is represented by a power series of η, then the η and η^2 terms drop out. The term of third degree exists only with certainty for the flow not fully developed.

The knowledge of the behavior of the exchange coefficient in the immediate vicinity of the boundary is of essential significance for the theory of heat exchange. In a recent paper about "The Influence of Flow near the Surface on the Turbulent Heat Exchange" the proportionality of the exchange coefficient with η^3 was accepted. (Mitteilungen aus dem Max-Planck-Institute für Strömungsforschung Nr. 3, 1950.) The small $\frac{A}{\mu}$ values given there for very small η distances are possibly too large since $\frac{A}{\mu}$ possibly increases by higher than the 3rd power of η. K. Elser in his paper, "Friction Temperature Fields in Turbulent Boundary Layers", postulates an essentially higher behavior of frictional turbulence near the surface. (Mitt. Inst. Thermodynamik ETH Zurich, H. 8 (1949).

For the representation of $\frac{A}{\mu}$ as a function of y or η we therefore need a function whose first and second derivative is 0 on the boundary. On the other hand, this function, at some distance from the boundary, must change asymptotically to the linear behavior of $k\eta$.

The function

$$\frac{A}{\mu} = k\left(\eta - \eta_1 \tanh\frac{\eta}{\eta_1}\right) \tag{12}$$

satisfies these two conditions. We will therefore use this equation as an expression for $\frac{A}{\mu}$.

The constant η_1 appearing in Eq (12) is a measure of the strength of the laminar boundary layer. η_1 must be such that the calculated velocities of the turbulent boundary flow coincide with the measured velocities (calculations are made by using Eq (12)).

The behavior of $\frac{A}{\mu}$ as given by Eq (12) is represented by Fig. 1 for $K = 0.4$ and $\eta_1 = 11$.[4] As we will show below, this value of η_1 leads to a value of 5.5 for the constant C of the logarithmic boundary law.

By using Eq (12) and considering the fact that in fully developed flow $\tau = \tau_0 (1 - \frac{y}{r})$ it follows from Eq (5)

$$\frac{d\left(\frac{u}{u^*}\right)}{d\eta} = \frac{1 - \frac{y}{r}}{1 + K(\eta + \eta_1 \tanh\frac{\eta}{\eta_1})} \,. \tag{13}$$

The integration of this equation unfortunately cannot be performed with the help of the familiar operations. We must therefore look for aids.

First of all, we can neglect the value of $\frac{y}{r}$ compared to 1 because we are dealing in this chapter with processes near the boundary. Furthermore, it is advisable to separate a term $\frac{1}{(1 + K\eta)}$ on the right side of Eq (13) in order to make possible, at least, the integration by parts. After carrying out this integration we then obtain:

$$\frac{u}{u^*} = \frac{1}{K} \ln(1 + K\eta) + f(\eta). \tag{14}$$

Here $f(\eta)$ is defined by the equation:

$$f(\eta) = \int_0^\eta \frac{K\eta_1 \tanh\frac{\eta}{\eta_1} d\eta}{(1 + K\eta - K\eta_1 \tanh\frac{\eta}{\eta_1})(1 + K\eta)} \,. \tag{15}$$

Also, the integration of Eq (15) is not practicable. However, we can replace, as an approximation, the integrand $f'(\eta)$ by the function

---

[4] As Fig. 1 shows, $A < \mu$ in the region $\eta <\approx 11$ and $A > \mu$ in the region $\eta > \approx 11$. The dimensionless boundary distance $\eta \approx 11$ is therefore a measure of the strength of that layer near the boundary in which the molecular friction outweighs the turbulent friction.

$$f_1' = \frac{C_1}{\eta}\left[e^{-\eta/\eta_1} + (b\eta - 1)\, e^{-b\eta}\right] \qquad (16)$$

through which the integration becomes possible. We than obtain for f_1 :

$$f_1 = C_1\left(1 - e^{-\eta/\eta_1} - \frac{\eta}{\eta_1}\, e^{-b\eta}\right) . \qquad (17)$$

Here constants C_1 and b are to be determined from the boundary condition.

If we replace f in Eq. (14) by the approximation f_1 as given in Eq. (17), then we obtain for high values of η (for which 1 is to be neglected compared to $K\eta$):

$$\frac{u}{u_*} = \frac{1}{K}\ln\eta + \frac{1}{K}\ln K + C_1 . \qquad (14a)$$

Comparing this equation with Eq (1) which is valid for high values of η , then it follows that $\frac{1}{K}\ln K + C_1 = C$.

Using the usual values for $K = 0.4$ and $C = 5.5$, we obtain $C_1 = 5.5 + 2.3 = 7.8$.

The value of the constant η_1 is determined from the condition that the integral of Eq. (15) reaches the value 7.8 by using high η values and $K = 0.4$. We have graphically integrated and determined Eq. (15) for various η_1 values in such a manner that the boundary value of 7.8 is obtained when $\eta = 11$.

The constant b was to be obtained from the boundary conditions of the wall shear stress. These conditions are essentially not violated if one uses $b = 0.33$. If we now introduce the above results into Eq (14), then we obtain as an approximation for the boundary law:

$$\frac{u}{u_*} = 2.5\ln(1 + 0.4\eta) + 7.8\left(1 - e^{-\eta/11} - \frac{\eta}{11}\, e^{-0.33\eta}\right) \qquad (18)$$

$\frac{u}{u^*}$ is represented in Fig. 1 for small η values and in Fig. 3 (as a function of log η) for somewhat large η values. The solid curves show the results of the graphical integration while the dotted curves give $\frac{u}{u^*}$ according to the approximate Eq (18). As one can see, no essential differences exist between the dimensionless velocities obtained by graphical integration and those obtained from the approximate solution. Somewhat larger differences exist at places between f' (solid) and f_1' (dotted), as is seen in Fig. 2. This deviation is meaningless inasmuch as one is not dependent on the approximate Eq (16) for any calculations in which the derivative of f is involved since the integrand of Eq (15) can be used directly.

Compared with Eq (1), our Eq (18) has the advantage of describing the turbulent shear stress for every η value in the region near the boundary. While $\frac{u}{u^*}$ goes to $-\infty$ with decreasing η as given by Eq (1), our Eq (18) in addition fulfills the condition of $u = 0$ when $\eta = 0$.

For very small finite values of η, it follows from Eq (18) that:

$$\frac{u}{u^*} = \eta$$

This is the linear increase in velocity in the laminar boundary layer. We achieve the same result from Eq (5) if we give A the value of 0. This linear increase extends to $\eta \approx 4$ (see Fig. 1). From there on, the dimensionless velocity increases less than linearly with η. This velocity deviates more and more from the straight line with increasing η and eventually becomes logarithmic (at about $\eta = 100$).

The smaller magnitudes of the velocity compared to the straight line relationship with η is caused by the appearance of turbulence. The influence of the turbulent friction is recognized not only by the ratio $\frac{A}{\mu}$ (Fig. 1), but also by the relationship

$$\frac{\tau_t}{\tau} = \frac{\frac{A}{\mu}}{1+\frac{A}{\mu}}, \tag{19}$$

which is represented in Fig. 2 by use of Eq. (12). As one recognizes from both figures, a noticeable turbulent friction is determinable only after $\eta = 4$, where the dimensionless velocity deviates from the straight line relationship with η. Where the transition into the logarithmic velocity distribution occurs (at about $\eta = 100$), the part of the turbulent friction amounts to over 98% of the total shear stress.

The observations as presented have only approximate validity since we do not know the exact manner of decay of the turbulent shear stress near the boundary. The velocity distribution represented by our Eq (18) should, however, not deviate essentially from actuality because the boundary conditions for the mixing coefficient as well as velocity, both on the boundary and at greater distance from the boundary, were correctly satisfied.

The experimental investigation of the boundary law for small values of η is no simple problem because the velocity detectors (pitot tubes, hot wires) close to the surface and at very low velocities give erroneous indications, the sufficiently exact determination of which presents great difficulties. Measurements of velocity under conditions of small η values, which the author carried out in an earlier work[5], are represented in Fig. 3. As one can see, most of the measured points lie near the calculated curve. Somewhat larger deviations appear in hot-wire measurements carried out very close to the surface, and these measured velocities tend to be too low.

---

[5] H. Reichardt, Die Wärmeübertragung in turbulenten Reibungsschichten. Z. angew. Math. Mech 20 (1940), S. 297.

4. The Center Law

Since in the middle part of a canal or pipe all processes are symmetrical with respect to the center plane and/or axis, it is advisable to locate the origin of the coordinate system in the center plane or axis. Let the distance from this origin be z. z varies from r to $-r$. The boundary may be located to the left of the center at a distance $z = r$. We represented the distribution of velocity in the vicinity of this boundary by the equation mentioned above. Therefore $z = r - y$ or $y = r - z$.

In the middle region the molecular viscosity can be neglected when compared to the turbulent exchange. If we replace $\frac{dy}{r}$ by $\frac{dz}{r}$ in our fundamental equation (Eq 5), then we obtain

$$\frac{d\left(\frac{u}{u_*}\right)}{d\left(\frac{z}{r}\right)} = \frac{\frac{\tau}{\tau_o}}{\frac{A}{\mu\,\eta_r}} . \tag{20}$$

Our experiments give information about the dimensionless exchange coefficient $\frac{A}{\mu\eta_r}$. We could determine the exchange coefficient fairly accurately in the middle region (See Figs. 4 and 5)[6] through direct measurement of the differential quotient of the stagnation pressure by using a double pitot-tube. These experiments may be approximately and uniformly represented by the following equation:

$$\frac{A}{\mu\,\eta_r} = \frac{K}{3}\left[0.5 + \left(\frac{z}{r}\right)^2\right]\left[1 - \left(\frac{z}{r}\right)^2\right] . \tag{21}$$

---

[6] In Fig. 4 $\phi = \frac{\bar{u}}{u_{max}}$. The measurements were made in the middle vertical cross-section of a rectangular canal 24.6 cm in height and 98 cm in width.

If we introduce this relation into Eq (20) and observe that in fully ...veloped flow $\frac{\tau}{\tau_0} = 1 - \frac{y}{r} = \frac{z}{r}$, it follows:

$$- \frac{2}{3} K \frac{u}{u^*} = \int \frac{d\left(\frac{z}{r}\right)^2}{\left[0.5 + \left(\frac{z}{r}\right)^2\right]\left[1 - \left(\frac{z}{r}\right)^2\right]} + const. \tag{22}$$

The integration gives

$$\frac{u}{u^*} = \ln\left[\frac{1 - (z/r)^2}{0.5 + (z/r)^2}\right] + const. \tag{23}$$

We determine the constants for the center plane and/or axis, where $\frac{z}{r} = 0$ and $u = u_m$ by

$$\frac{u_m - u}{u^*} = \frac{1}{K} \ln\left[\frac{1 + 2(z/r)^2}{1 - (z/r)^2}\right] . \tag{24}$$

This formula represents the entire velocity distribution of flow for the cross-section except for the thin layers close to the boundaries in which the molecular friction plays an essential part. In Eq (24) no distance to the boundary is involved and only the distance z from the center appears. This distance represents the plane of symmetry and/or axis of symmetry of the velocity profile, and therefore we have here to do with a genuine "Center Law."

To test Eq (24) the author carried out measurements of velocity (see footnote 6). These measurements were presented in the form prescribed by Eq (24). As Fig. 6 shows (in which instead of the natural logarithm the logarithm to the base 10 appears) the measured points lie on or in the vicinity of a straight line having a slope of 5.75 (this corresponds to a slope of $\frac{1}{K} = 2.5$ by using the natural logarithm). From the lower scale for $\frac{z}{r}$ we can see that the center law Eq (24) is valid past $\left(\frac{z}{r}\right) = 0.9$; that is, into the close vicinity of the boundaries.

For small values of $\frac{z}{r}$ the logarithm in Eq (24) may be replaced by a series, and one can write

$$\phi = 1 - \frac{3}{K \frac{u_m}{u^*}} \left(\frac{z}{r}\right)^2 . \tag{25}$$

Thus we obtain for the middle part a parabolic form of the velocity profile.

In Fig. 4, which shows the distribution of velocity $\phi = \frac{u}{u_m}$ for $u = 15.2$ cm/sec., the parabolic profile of Eq (25) is shown dotted. As one can see, the parabola and the top of the measured velocity profile are almost identical.

The parabolic shape of the top of the profile is due to the fact that the friction coefficient barely changes in the middle part of the cross-section of flow (for small $\frac{z}{r}$ it follows from Eq (21) $\frac{A}{\mu \eta_r} \approx \frac{K}{6}$). This condition is also recognized directly from the actual linear behavior of the velocity gradient in the middle cross-section of flow. Because $\tau = A \frac{d\bar{u}}{dz} = \tau_0 \frac{z}{r}$, the linearity of $\frac{d\bar{u}}{dz}$ is an indication of the constancy of the exchange coefficient.

It is typical for the turbulent profiles that with increasing distances from the center the velocity gradient first increases slowly, as can be seen in Fig. 4. In the center region $\left(\left|\frac{z}{r}\right| < 0.7\right)$ the measured points $\left|\frac{d\phi}{dz}\right|$ lie below the observed linear relationship shown as a dotted line. This variation of the profile from a straight line with increasing z , which manifests itself in the flattening of the velocity profile compared to the parabola, occurs because of the increase in the value of the exchange coefficient $\left(A \sim \frac{z}{r} \Big/ \frac{d\phi}{dz}\right)$ (see Fig. 5). This coefficient has its maximum when $\frac{z}{r} \approx 0.50$ as Nikuradse has already determined (see above). Here lies, therefore, also the minimum of the $\frac{d^2\phi}{dz^2}$ profile.

We will now represent the calculated velocity distribution Eq (24) as a function of a boundary distance and for this purpose introduce the distance y from the left boundary into Eq (24). Since $y = r-z$, we then obtain:

$$\frac{u - u_m}{u^*} = \frac{1}{K}\left[\ln\frac{y}{r} + \ln\frac{1+\frac{z}{r}}{1+2\left(\frac{z}{r}\right)^2}\right]. \tag{26}$$

If here we omit the second term, we then obtain the center law in its present form.

For further transformation of Eq (26) we define a dimensionless additional velocity $\frac{u_i}{u^*}$ by the following equation:

$$\frac{u_i}{u^*} = \frac{1}{K}\ln\left[\frac{0.5\left(1-\frac{z}{r}\right)}{1+2\left(\frac{z}{r}\right)^2}\right]. \tag{27}$$

Furthermore, introducing $\eta_r = \frac{r u^*}{\nu}$ into Eq (26) and denoting the value of u in the center by u_{im} it follows:

$$\frac{u}{u^*} - \frac{1}{K}\ln\eta - \frac{u_i}{u^*} = \frac{u_m}{u^*} - \frac{1}{K}\ln\eta_r - \frac{u_{im}}{u^*}. \tag{28}$$

On the right side of this equation are the constants which the individual terms on the left side reach in the center of the pipe or canal. Since the right side of Eq (28) is constant, we can also write

$$\frac{u}{u^*} = \frac{1}{K}\ln\eta + \frac{u_i}{u^*} + C = \frac{1}{K}\ln\left[\eta\,\frac{1.5\left(1+z/r\right)}{1+2\left(z/r\right)^2}\right] + C \tag{29}$$

where C denotes a constant to be determined experimentally.

Through the introduction of the dimensionless boundary distance η into our center formula Eq (24) we arrive at an equation which is different from the conventional boundary law equation by the additional term $\frac{u_i}{u^*}$. This term, which depends only on the coordinate $\frac{z}{r}$ and/or $\frac{y}{r}$ but not on u^* or η, reflects the deviation of the velocity distribution from the logarithmic profile. If one sets $K = 0.4$ into Eq (27), then $\frac{u_i}{u^*}$ takes the form shown in Fig. 5.

As Fig. 5 shows, the additional velocities are small. The maximum value of $\frac{u_i}{u^*}$, which lies at $y \approx 0.78$, amounts to 1.28. From there on $\frac{u_i}{u^*}$ decrease rapidly until it reaches the value 1.01 in the center. This behavior is naturally only valid for the case of the fully developed flow with pressure drop as treated here. If one would calculate a corresponding function for the boundary layer of the smooth plate, then one would (judging from the measurement of Schultz-Grunow[7]) obtain twice as high values of $\frac{u_i}{u^*}$. These higher additional velocities obviously have their foundations in the decay of the turbulent exchange at the transition of the boundary layer flow into the outer potential motion.

The peculiar form of the function $\frac{u_i}{u^*}$ explains the well known slightly curved sections of the velocity distribution which the test data, within the cross-section of flow, indicate when plotted semi-logarithmically. These deviations from the logarithmic straight line disappear when instead of $\frac{u}{u^*}$, $\frac{u-u_i}{u^*}$ is plotted as a function of $\log \eta$. This is brought out in Fig. 7, where the velocity measurements appearing in Fig. 6 are repeatedly plotted in the manner just described. In contrast to the $\frac{u}{u^*}$ test data, the $\frac{u-u_i}{u^*}$ points form an entirely straight line, indicating the usefulness of the formula for $\frac{u_i}{u^*}$.

As Fig. 7 shows, the points $\frac{u-u_i}{u^*}$ lie somewhat below the straight dotted line which has the slope $\frac{2.3}{\kappa} = 5.75$ and cuts the abscissa at the point $C = 5.5$. We have to withhold an exact determination of C and κ from the measurements at hand because the u^* values determined from the pressure gradient are too inexact for this problem[8].

---

[7] F. Schultz-Grunow, Neues Reibungswiderstandsgesetz für glatte Platten. Lufo 17 (1940), S. 239.

[8] The question of whether and to what degree the constants κ and C depend on the cross-section of flow can only be cleared up through further experiments.

At present we can only say that the use of the term $\frac{u_i}{u^*}$ has fundamentally introduced a certain change in the values of the constants C and K. Looking forward, one can retain the value $K = 0.4$ and use a reduced value of C.

Also, in the new plot there is still a certain scattering of data present as is indicated in Fig. 7. These undulations are only partly accountable through errors in measurement and/or mean value formation. Because of certain deficiencies of the experimental set-up (disturbances in the upstream flow) at times the velocity profiles were not entirely symmetrical. These disturbances affected the measurements. Something else is still to be reflected upon.

Our measurements represented in Fig. 5 of $\frac{A}{\mu \eta_r}$ show a certain dependence of this function on the Reynold's number and/or η_r. If this observation should be true, then our simple equation (21) (whose right side is independent of η_r) would be fundamentally inadequate for an exact representation of the turbulent profile. Although extraordinarily important in principle, this question should, however, play no role, since even through such a considerable change of the theory as it is indicated in our expression (21) only the following fact could be brought out: namely, that the deviations from the logarithmic velocity distribution in the middle region of the cross-section of flow are minor.

We have yet to answer the important question: why is the logarithmic shape of the velocity profile so dominant even though the logarithmic law should, according to hypothesis, be valid only for the direct vicinity of the boundary? This peculiar condition rests in the fact that in the old theory two factors were neglected which, when they are considered, cancel each other in part. The one factor is the decrease of the shear stress with the distance from the boundary, and the other is the deviation of the exchange coefficient from the assumed linear increase at the boundary.

To show this, we introduce into our fundamental equation (5) (in which 1 compared to $\frac{A}{\mu}$ is to be neglected) $\frac{\tau}{\tau_0} = 1 - \frac{y}{r}$ (instead of the former value 1), as well as

$$\frac{A}{\mu \eta_r} = K \frac{y}{r} \left(1 - \frac{y}{r}\right) \tag{30}$$

instead of the formerly used expression $K \frac{y}{r}$. We then obtain

$$\frac{d\left(\frac{u}{u^*}\right)}{d\left(\frac{y}{r}\right)} = \frac{1 - \frac{y}{r}}{K \frac{y}{r}\left(1 - \frac{y}{r}\right)} . \tag{31}$$

Since here $1 - \frac{y}{r}$ can be abbreviated, this equation means that the logarithmic distribution of velocity would be exactly valid to the center of the cross-section of flow if Eq (30) were valid for the exchange coefficient. In any case, the deviations of the actual distribution of velocity from the logarithmic profile can be traced back to the departures of the measured values $\frac{A\mu}{\eta_r}$ from the function described by Eq. (30).

To be able to evaluate these differences we have also plotted the function of Eq. (30) in Fig. 5 (see the dotted parabola). As one can see, this parabola shows the tendency of the behavior of the exchange coefficient much better than the constantly increasing straight line $K \frac{y}{r}$. In spite of considerable deviations in spots from the measured points, the parabolic behavior in the vicinity of the boundary represents a proportionally favorable approach to the actuality (reaching about as far as $\frac{y}{r} = 0.15$). But at this distance from the boundary the flow has already reached a considerable velocity ($u \approx 0.7\, u_{max}$). The development of the velocity is completed for the most part in a zone in which the logarithmic distribution is fairly valid.

The rest of the development of the velocity ($0.7 < \frac{u}{u_m} < 1$) extends over a great range ($0.15 < \frac{y}{r} < 1$) . In the middle cross-section of flow the velocity profile is then relatively flat. But the smaller the velocity gradient is, the weaker also is the influence of the value of the exchange coefficient on the rest of the velocity behavior. We understand, therefore, that the greater deviations of the measured values $\frac{A}{\mu \eta_r}$ from those represented by Eq. (30) (which appear towards the inside) have then a small effect.

As we have already shown, the deviations from the logarithmic distribution take place in the sense of additive velocities. The actual velocities are therefore higher than those of the logarithmic profile because the actual turbulent friction coefficient is, for the most part of the cross-section of flow, smaller than the friction coefficient of Eq. (30) on which the logarithmic law is based. As one can see from Fig. 5, the measured $\frac{A}{\mu \eta_r}$ values lie below the parabola representing Eq. (30) up to a surface distance of $\frac{y}{r} = 0.78$. The additional velocity $\frac{u_i}{u^*}$ therefore has its maximum at $\frac{y}{r} = 0.78$. Then $\frac{u_i}{u^*}$ decreases again for still greater distances from the surface until the center is reached because the actual exchange coefficient is greater in this region than the coefficient of the logarithmic profile represented by Eq. (30).

5. FORMULA FOR THE ENTIRE CROSS-SECTION

We have derived a formula in Section 3 (Eq. (18)) which represents the distribution of velocity reaching into the laminar boundary layer. This distribution of velocity extends internally to the logarithmic pxfile.

In Section 4 we have shown that the logarithmic profile is not exactly valid in the middle region of the cross-section of flow, and we have calculated additional velocities $\frac{u_i}{u^*}$ appearing there (Eq. (27)). These additional velocities are defined so that instead of $\frac{u}{u^*}$, $\frac{u-u_i}{u^*}$ obeys the logarithmic law.

We can therefore extend the region of validity of our boundary Eq. (18) to the entire cross-section of flow since we substituted $\frac{u-u_i}{u^*}$ for $\frac{u}{u^*}$ in Eq. (18). If we discard the still somewhat uncertain numerical values for the constants K, η_0, and b as well as the value of the term $C_1 = C - \frac{1}{K}\ln K$ which is influenced by the shape of the cross-section of flow, we then obtain

$$\frac{u-u_i}{u^*} = \frac{1}{K}\ln(1+K\eta) + C_1\left(1 - e^{-\eta/\eta_1} - \frac{\eta}{\eta_1}e^{-by}\right). \tag{32}$$

Further, if we introduce $\frac{u}{u^*}$ from Eq. (27) then we obtain as a final valid formula for the turbulent distribution of velocity for the entire cross-section:

$$\frac{u}{u^*} = \frac{1}{K}\ln\left[(1+Ky)\frac{1.5(1+z/r)}{1+2(z/r)^2}\right] + C_1\left(1-e^{-\eta/\eta_1} - \frac{\eta}{\eta_1}e^{-by}\right). \tag{33}$$

As one can easily verify, this equation transforms into the boundary law Eq. (18) for small distances from the boundary ($\frac{z}{r} \approx 1$). Otherwise the cross-section Eq. (29) follows from Eq. (33) for high η values.

Submitted Aug. 28, 1950.

ACKNOWLEDGMENT

This translation was sponsored by the Air Force Cambridge Research Center under Contract No. AF-19(604) - 421.

Diesen beiden Anforderungen wird nun die Funktion

$$\frac{A}{\mu} = \varkappa\left(\eta - \eta_L \operatorname{Tang}\frac{\eta}{\eta_L}\right) \qquad (12)$$

gerecht. Wir werden daher diese Gleichung als Ansatz für A/μ benutzen.

Die in (12) auftretende Konstante η_L ist ein Maß für die „Stärke der laminaren Wandschicht". η_L ist so vorzugeben, daß die mit Hilfe von (12) berechneten Geschwindigkeiten der turbulenten Wandströmung mit den gemessenen Geschwindigkeiten übereinstimmen.

Der durch Formel (12) beschriebene Verlauf von A/μ ist in Bild 1 dargestellt und zwar für $\varkappa = 0{,}4$ und $\eta_L = 11$[1]). Wie wir noch weiter unten darlegen werden, führt dieser Wert von η_L zu dem Werte 5,5 der Konstanten c des logarithmischen Wandgesetzes (1).

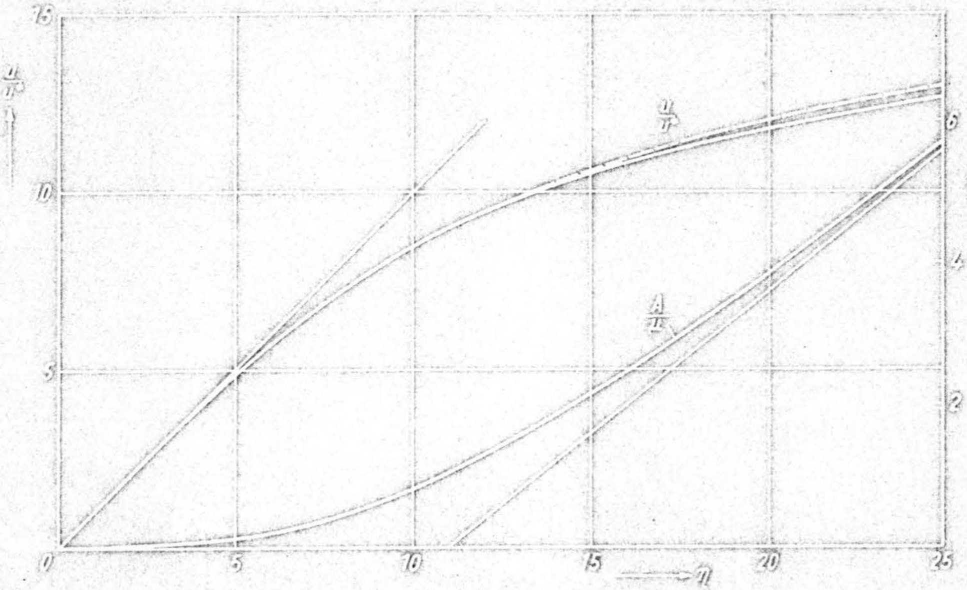

Bild 1

Bei Verwendung von (12) und unter Beachtung der Tatsache, daß in ausgebildeter Strömung $\tau = \tau_0\left(1 - \frac{y}{r}\right)$ ist, folgt aus (5)

$$\frac{d\left(\frac{u}{v^*}\right)}{d\eta} = \frac{1 - \frac{y}{r}}{1 + \varkappa(\eta - \eta_L \operatorname{Tang}\eta/\eta_L)} \qquad (13).$$

Die Quadratur dieser Gleichung ist leider nicht mit Hilfe der bekannten Rechenoperationen auszuführen. Wir müssen daher nach Aushilfen suchen.

Zunächst können wir im Zähler y/r gegenüber 1 vernachlässigen, da wir es ja in diesem Kapitel ausschließlich mit wandnahen Vorgängen zu tun haben. Ferner empfiehlt es sich, auf der rechten Seite von (13) ein Glied $1/(1 + \varkappa\eta)$ abzuspalten, weil dadurch wenigstens eine Teilintegration möglich wird. Nach Ausführung dieser Integration erhalten wir dann

$$\frac{u}{v^*} = \frac{1}{\varkappa}\ln(1 + \varkappa\eta) + f(\eta) \qquad (14).$$

Hier ist $f(\eta)$ durch die Gleichung definiert

$$f(\eta) = \int_0^\eta \frac{\varkappa\,\eta_L \operatorname{Tang}\eta/\eta_L\,d\eta}{(1 + \varkappa\eta - \varkappa\eta_L \operatorname{Tang}\eta/\eta_L)(1 + \varkappa\eta)} \qquad (15).$$

Auch die Quadratur von (15) ist nicht ausführbar. Wir können aber den Integranden $f'(\eta)$ näherungsweise durch die Funktion

$$f_1 = \frac{c_1}{\eta_1}\left(e^{-\eta/\eta_1} + (b\eta - 1)\,e^{-b\eta}\right) \qquad (16)$$

[1]) Wie Bild 1 zeigt, ist $A < \mu$ im Bereich $\eta < \approx 11$ bzw. $A > \mu$ im Gebiet $\eta > \approx 11$. Der dimensionslose Wandabstand $\eta_L \approx 11$ ist daher ein Maß für die Stärke derjenigen wandnahen Schicht, in der die molekulare Reibung die turbulente Reibung überwiegt.

rohres konnten wir die Austauschgröße vor allem für den mittleren Bereich ziemlich genau bestimmen (s. die Bilder 4 und 5)[6]. Diese Experimente lassen sich näherungsweise durch folgende Gleichung einheitlich darstellen

$$\frac{A}{\rho v^* r} = \frac{\varkappa}{3}\left(0{,}5 + \left(\frac{z}{r}\right)^2\right)\left(1 - \left(\frac{z}{r}\right)^2\right) \qquad (21).$$

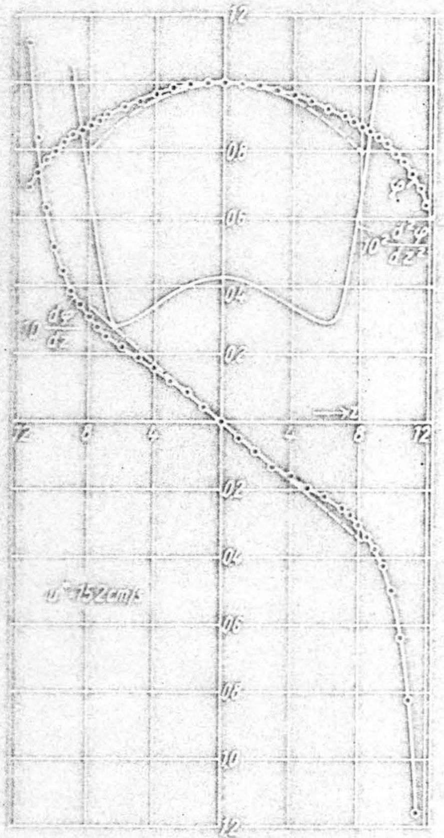

Bild 4

Führen wir diese Beziehung in (20) ein und beachten, daß in ausgebildeter Strömung $\frac{\tau}{\tau_0} = 1 - \frac{y}{r} = \frac{z}{r}$ ist, so folgt hieraus

$$-\frac{2}{3}\varkappa\frac{u}{v^*} = \int \frac{d\left(\frac{z}{r}\right)^2}{\left(0{,}5 + \left(\frac{z}{r}\right)^2\right)\left(1 - \left(\frac{z}{r}\right)^2\right)} + \text{konst} \qquad (22).$$

Die Integration ergibt

$$\varkappa\frac{u}{v^*} = \ln\left(\frac{1 - \left(\frac{z}{r}\right)^2}{0{,}5 + \left(\frac{z}{r}\right)^2}\right) + \text{konst} \qquad (23).$$

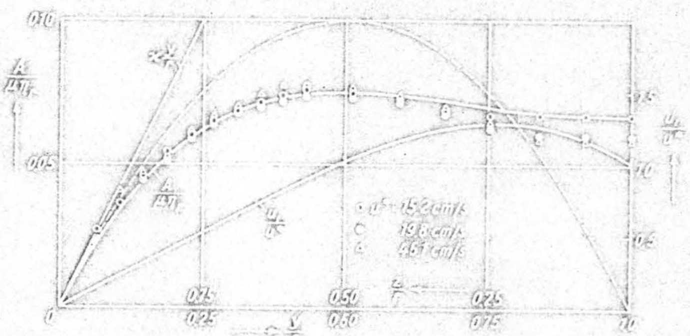

Bild 5

Die Konstante bestimmen wir für die Mittelebene bzw. Achse, wo $\frac{z}{r} = 0$ und $u = u_m$ ist:

$$\frac{u_m - u}{v^*} = \frac{1}{\varkappa}\ln\left(\frac{1 + 2\left(\frac{z}{r}\right)^2}{1 - \left(\frac{z}{r}\right)^2}\right) \qquad (24).$$

Diese Formel bezieht sich auf den gesamten Strömungsquerschnitt, ausgenommen die unmittelbar an den Wänden liegenden dünnen Schichten, in denen die molekulare Reibung eine wesentliche Rolle spielt. Da in Gl. (24) kein Wandabstand, sondern nur der Abstand z von der Mitte eingeht, die die Symmetrieebene bzw. Symmetrieachse des Geschwindigkeitsprofiles darstellt, haben wir es hier mit einem echten „Mittengesetz" zu tun.

Zur Prüfung der Formel (24) hat der Verfasser Geschwindigkeitsmessungen ausgeführt (s. Fußnote 6). Diese Messungen wurden in der durch Gl. (24) vorgeschriebenen Form aufgetragen. Wie Bild 6 zeigt (in dem statt des natürlichen Logarithmus der Zehnerlogarithmus erscheint) liegen die Meßpunkte auf bzw. in der Nähe einer Geraden mit der Neigung 5,75 (das entspricht einer Neigung von $\frac{1}{\varkappa} = 2{,}5$ bei Verwendung des natürlichen Logarithmus). An dem

Hier sind die Konstanten c_1 und b aus den Grenzbedingungen zu ermitteln.

Ersetzen wir in Gl. (14) f durch die in (17) dargestellte Näherungslösung f_1, so erhalten wir für hohe η (bei denen 1 gegenüber $\varkappa\eta$ zu vernachlässigen ist)

$$\frac{u}{u^*} = \frac{1}{\varkappa} \ln \eta + \frac{1}{\varkappa} \ln \varkappa + c_1 \qquad (14a).$$

Vergleichen wir diese Formel mit der für hohe η geltenden Gl. (1) so folgt, daß

$$\frac{1}{\varkappa} \ln \varkappa + c_1 = c$$

gesetzt werden muß. Unter Verwendung der üblichen Zahlenwerte $\varkappa = 0{,}4$ und $c = 5{,}5$ erhalten wir dann $c_1 = 5{,}5 + 2{,}3 = 7{,}8$.

Der Wert der Konstanten η_1 ergibt sich aus der Bedingung, daß das Integral der Gl. (15) bei Verwendung von $\varkappa = 0{,}4$ für hohe η den Wert 7,8 erreicht. Wir haben Gl. (15) für verschiedene η_1-Werte graphisch integriert und festgestellt, daß der geforderte Grenzwert 7,8 erhalten wird, wenn man $\eta_1 = 11$ setzt.

Die Konstante b war aus den Grenzbedingungen der Wandschubspannung zu ermitteln. Diese werden nicht wesentlich verletzt, wenn man $b = 0{,}33$ setzt.

Führen wir nun die vorstehenden Ergebnisse in Gl. (14) ein, so erhalten wir als Näherungsformel für das Wandgesetz:

$$\frac{u}{u^*} = 2{,}5 \ln (1 + 0{,}4\,\eta) + 7{,}8 \left(1 - e^{-\eta/11} - \frac{\eta}{11}\, e^{-0{,}33\,\eta}\right) \qquad (18).$$

Der Verlauf von u/u^* ist für kleinere η-Werte in Bild 1 und für etwas größere η in Abb. 3 dargestellt (und zwar hier als Funktion von $\log \eta$). Die ausgezogenen Kurven zeigen das Ergebnis der graphischen Integration, während die gestrichelten Kurvenzüge den u/u^*-Verlauf nach der Näherungsformel (18) wiedergeben. Wie man sieht, bestehen zwischen den durch graphische Integration und den durch Näherungsrechnung ermittelten dimensionslosen Geschwindigkeiten an keiner Stelle wesentliche Unterschiede. Etwas größere Differenzen bestehen stellenweise zwischen f'' (ausgezogen) und f_1'' (gestrichelt), wie man aus Bild 2 erkennt. Diese Abweichung ist aber insofern bedeutungslos, als man ja für irgendwelche Rechnungen, in die die Ableitung von f eingeht, nicht auf die Näherungsformel (16) angewiesen ist, sondern den Integranden von Gl. (15) unmittelbar verwenden kann.

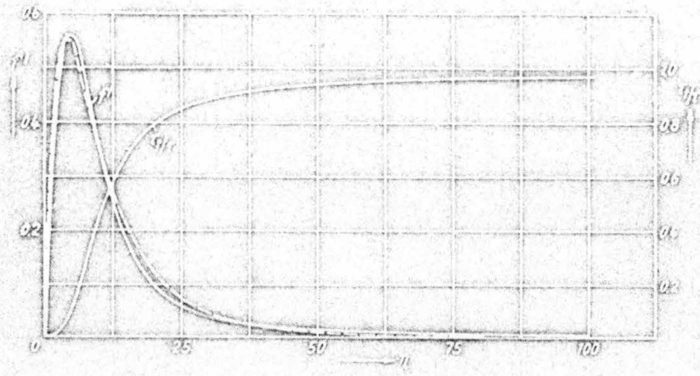

Bild 2

außer an A/μ (Bild 1) auch an dem Verhältnis

$$\frac{\tau_t}{\tau} = \frac{\frac{A}{\mu}}{1+\frac{A}{\mu}}$$

das unter Verwendung von Gl. (12) in Bild 2 dargestellt ist. Wie man aus B erkennt, ist eine nennenswerte turbulente Reibung erst ab $\eta = 4$ feststellbar, w bleiben der dimensionslosen Geschwindigkeit gegenüber dem geradlinigen Dort, wo der Übergang in die logarithmische Geschwindigkeitsverteilung bei $\eta = 100$), beträgt der Anteil der turbulenten Reibung an der gesamte über 98%.

Die vorstehenden Betrachtungen haben selbstverständlich nur näherun da wir die genaue Gesetzmäßigkeit des Abklingens der turbulenten Scheinrei nicht kennen. Formel (18) dar digkeitsverlauf der Wirklichkei abweichen, da d gen für die An für die Geschwi der Wand als au fernung von de füllt wurden.

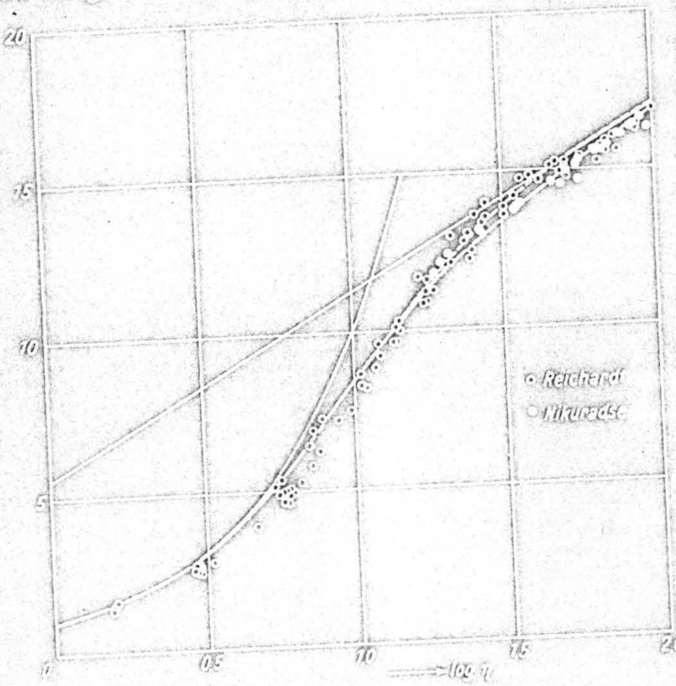

Bild 3

Die exper des Wandgesetz kein einfaches P schwindigkeitss chen, Hitzdraht nähe und bei schwindigkeiten ben, deren hinr mittlung groß bereitet. Solche ten durchgefüh keitsmessungen im Rahmen eine durchgeführt. In dargestellt. Wi die meisten Meß der gerechneten Kurve. Etwas größere Abweichungen treten lediglich bei d Wandabständen durchgeführten Hitzdrahtmessungen auf und zwar in dem messenen Geschwindigkeiten zu klein sind.

4. Das Mittengesetz

Da im mittleren Teil eines Kanales oder Rohres alle Vorgänge symm ebene bzw. Achse verlaufen, empfiehlt es sich, den Ursprung des Koordin Mittelebene bzw. in die Achse zu verlegen. Der Abstand von diesem Urspru von r bis $-r$. Links von der Mitte im Abstande $z = r$ möge sich die Wand Nähe wir soeben die Geschwindigkeitsverteilung dargestellt haben. Es ist $\eta = r - z$.

Im mittleren Bereich kann die molekulare Zähigkeit gegenüber dem tausch vernachlässigt werden. Führen wir noch $-dz/r$ statt $d\eta/r$ in unsere ein, so erhalten wir

$$\frac{d\left(\frac{u}{v^*}\right)}{d\left(\frac{z}{r}\right)} = \frac{\frac{\tau}{\tau_0}}{\frac{A}{\mu\eta_r}}$$

Über die dimensionslose Austauschgröße $A/\mu\eta_r$ geben unsere Versuch unmittelbare Messung des Differentialquotienten des Staudruckes mit Hilfe

[1]) H. Reichardt, Die Wärmeübertragung in turbulenten Reibungsschichten. 20 (1940), S. 297.

zichten, da die aus dem Druckgefälle bestimmten v^*-Werte …
Wir können zunächst nur sagen, daß das Auftreten des Glied… Änderung der Konstanten ϱ und $\varkappa$ zur Folge hat. Voraussich… beibehalten können und nur den c-Wert zu verringern brau…

Auch in der neuen Auftragung ist, wie aus Bild 7 hervo… der Meßpunkte vorhanden. Diese Schwankungen sind nur zu…

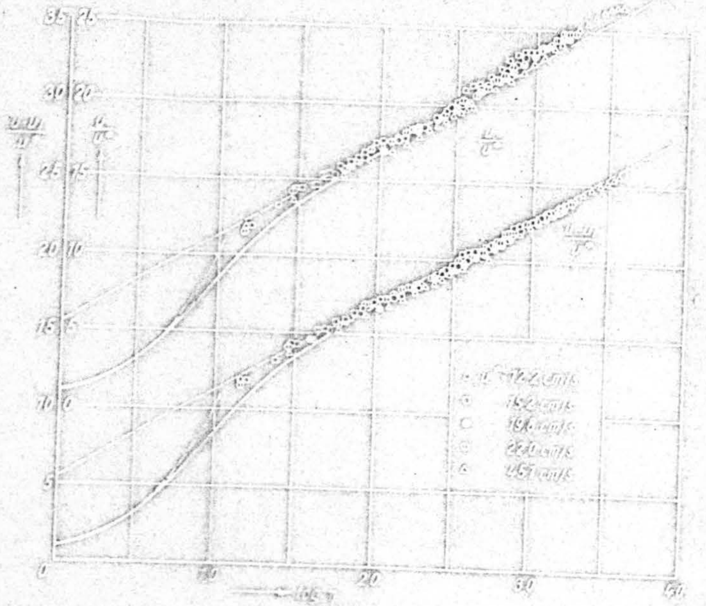

Bild 7.

keine Rolle spielen, da selbst durch eine so erhebliche Verä… Ansatz (21) zur Folge hatte, nur die Tatsache zur Darstellu… weichungen von der logarithmischen Geschwindigkeitsverte… mungsquerschnittes nur gering sind.

Wir haben nun noch die wichtige Frage zu beantworten… des Geschwindigkeitsprofiles so dominiert, obwohl das logar… gemäß nur für die unmittelbare Nähe der Wand gelten sollte… hat seinen Grund darin, daß in der alten Theorie zwei Fak… die, wenn man sie berücksichtigt, sich zum Teil gegenseitig… Abfall der Schubspannung mit dem Wandabstand, der ander… größe von dem angenommenen linearen Anstieg an der Wa…

Um das zu beweisen, setzen wir in unserer Grundgleic… zu vernachlässigen ist) $\frac{\tau}{\tau_0} = 1 - \frac{y}{r}$ (anstelle des früheren W…

$$\frac{A}{\mu \, v_*} = \varkappa \, \frac{y}{r}\left(1 - \frac{y}{r}\right)$$

anstelle des früher benutzten Ausdruckes $\varkappa \frac{y}{r}$. Wir erhalt…

$$\frac{d\left(\frac{u}{v^*}\right)}{d\left(\frac{y}{r}\right)} = \frac{1 - \frac{y}{r}}{\varkappa \frac{y}{r}\left(1 - \frac{y}{r}\right)}.$$

Da hier $\left(1 - \frac{y}{r}\right)$ gekürzt werden kann, besagt diese Gleich… schwindigkeitsverteilung bis zur Mitte des Strömungsquerschn… die Austauschgröße die Funktion (30) Gültigkeit hätte. Jedenf… tatsächlichen Geschwindigkeitsverteilung vom logarithmische… gemessenen Werte $A/\mu \, v_*$ von der durch Formel (30) beschriebene…

¹) Die Frage, ob und in welchem Ausmaß die Konstanten $\varkappa$ und … schnittes abhängen, kann nur durch weitere Versuche geklärt werden.

Für kleine z/r läßt sich der Logarithmus in (24) durch eine Reihe ersetzen und ma schreiben

$$\varphi = 1 - \frac{3}{\varkappa\, u_m} \frac{}{u^*} \left(\frac{z}{r}\right)^2$$

Wir erhalten also für den mittleren Teil eine parabolische Form des Geschwindigkeitsp

In Bild 4, das die Geschwindigkeitsverteilung $\varphi = \frac{u}{u_{max}}$ für $u^* = 15{,}2$ cm/s zeigt, Parabelprofil der Formel (25) gestrichelt eingezeichnet. Wie man sieht, besteht zw dieser Parabel und der Kuppe des gemessenen Geschwindigkeitsprofils eine innige Beru

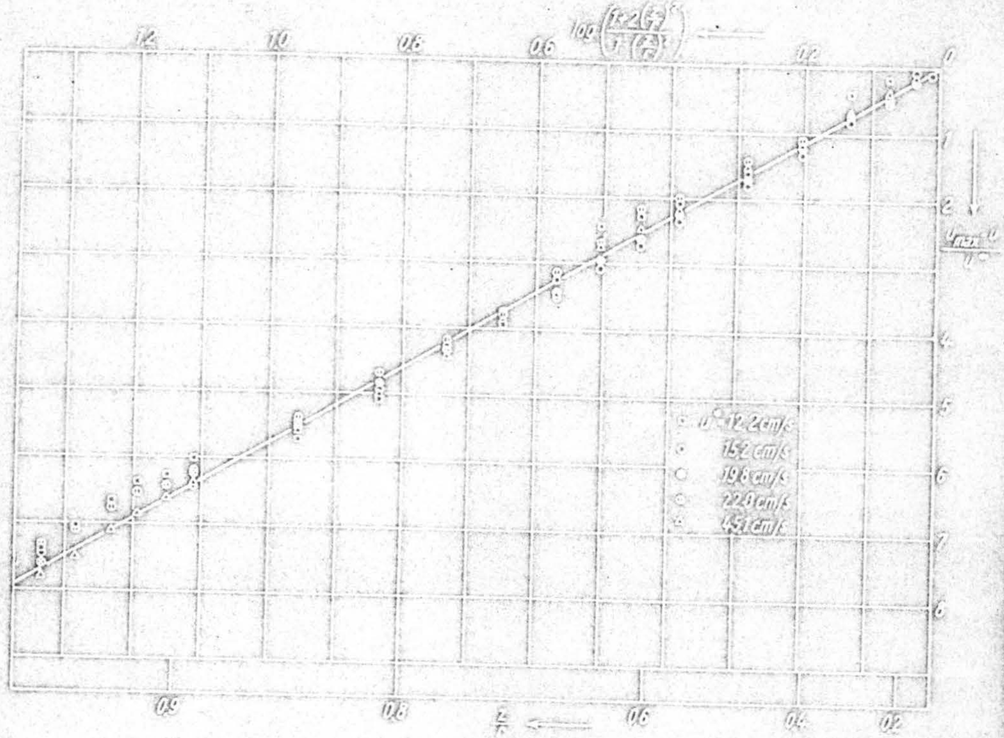

Bild 6

Die parabolische Gestalt der Profilkuppe hat ihren Grund darin, daß sich der tu lente Reibungskoeffizient im mittleren Teil des Strömungsquerschnittes kaum verä $\left(\text{für kleine } \frac{z}{r} \text{ folgt aus (21) } \frac{A}{\rho\, u_t} \approx \frac{\varkappa}{6}\right)$. Diesen Sachverhalt erkennt man auch unmitt aus dem praktisch linearen Verlauf des Geschwindigkeitsgradienten im mittleren Ström querschnitt. Denn da $\tau = A \frac{d\bar{u}}{dz} = \tau_0 \frac{z}{r}$ ist, ist die Linearität von $\frac{d\bar{u}}{dz}$ ein Kennzeichen die Konstanz der Austauschgröße.

Es ist typisch für die turbulenten Profile, daß der Anstieg des Geschwindigkeitsgradie mit wachsender Entfernung von der Mitte zunächst nachläßt, wie man aus Bild 4 ers Im mittleren Bereich $\left(\frac{z}{r} < 0{,}7\right)$ liegen die Meßpunkte $\frac{d\varphi}{dz}$ unterhalb des gestrichelt ei zeichneten linearen Verlaufes, den man in der Mitte beobachtet. Dieses Nachlassen der P krümmung mit wachsendem z, das sich in einem Flacherwerden des Profiles gegenüber der P bel äußert, hat seinen Grund in dem Anstieg der Austauschgröße $\left(A \sim \frac{z}{r} \Big/ \frac{d\varphi}{dz}\right)$ (s. Bild Diese hat ihr Maximum bei $\frac{z}{r} \approx 0{,}5$, wie bereits Nikuradse (s. oben) festgestellt hat liegt daher auch das Minimum der Profilkrümmung $\frac{d^2\varphi}{dz^2}$.

Wir wollen nun die errechnete Geschwindigkeitsverteilung (24) als Funktion eines W abstandes darstellen und führen zu diesem Zweck den Abstand y von der linken Wand ein